Enhancing quantum efficiency and performance parameters in silicon solar cells through integrated plasmonic nanoparticles and graphene grating structures

DONYA ADABI[1], MOHAMMAD REZA SHAYESTEH[1,*], MOHAMMAD REZA MOSLEMI[2], SAEEDEH HASHEMIAN[3]
[1]*Department of Electrical Engineering, Yazd Branch, Islamic Azad University, Yazd, Iran*
[2]*Department of Electrical Engineering, Zarghan Branch, Islamic Azad University, Zarghan, Iran*
[3]*Chemistry Department, Yazd Branch, Islamic Azad University, Yazd, Iran*

In this study, we introduce an innovative silicon solar cell design aimed at enhancing both current density and overall efficiency. This novel architecture features a unique combination of alternating or window-shaped doping profiles at the top layer, complemented by a graphene grating layer situated in the middle, and strategically positioned gold nanoparticles between the doping and grating layers. We conducted a comprehensive performance evaluation of various solar cell configurations, including a basic silicon solar cell, cells with window doping, grating, nanoparticles, and a combination of doping, nanoparticles, and grating. Our findings reveal that the proposed structure, with its synergistic integration of grating, window-shaped doping, and nanoparticles, significantly amplifies the electric field strength within the active region. This enhancement leads to a remarkable improvement in solar cell performance, highlighted by a quantum efficiency value reaching up to 81%, a short-circuit current density of 35 mA/cm^2, a fill factor (FF) of 83%, and an open-circuit voltage (VOC) of 0.66 V. These results underscore the potential of the proposed design in pushing the boundaries of silicon solar cell efficiency and performance.

(Received October 11, 2023; accepted April 8, 2024)

Keywords: Solar cell, Plasmonic, Doping, Efficiency

1. Introduction

The conversion of daylight into energy via solar cells, a process grounded in the photovoltaic effect, remains a cornerstone of renewable energy research [1]. Discovered by Bequerel in 1839, the photovoltaic effect involves the excitation of electrons in response to light, a phenomenon facilitated by the semiconductor material's p-n junction [1]. However, maximizing solar cell efficiency necessitates optically thick photovoltaic layers for effective light absorption, a challenge mitigated by the advent of plasmonic nanostructures [2-5]. These structures, particularly when closely coupled to semiconductors, enhance absorption in ultrathin films, thereby offering a pathway to high-efficiency, reduced-material solar cells.

Localized surface plasmons, the resonant oscillations of conductive electrons at the nanoparticle interface under light excitation, significantly augment light absorption and scattering within solar cells. These phenomena, which vary with the size and shape of the nanoparticles, can lead to enhanced photocurrent collection [6-7]. Research has elucidated the potential of sub-wavelength light trapping structures, including both metallic and dielectric nanostructures, to induce effective light trapping and scattering, further advancing thin-film solar cell technology [8-11].

Metallic nanoparticles, notable for their ability to sustain localized surface plasmons, are particularly effective in extending the optical path within solar cells, thereby improving their absorption and overall efficiency [12-31]. These enhancements stem from both far-field and near-field effects, which respectively refer to the scattering enhancement and local electric field amplification near the semiconductor material. Additionally, the integration of nanostructured metallic films on the rear side of PV layers can couple light into surface plasmon polariton (SPP) modes, further boosting cell performance [32-35].

This paper introduces a novel silicon solar cell architecture that incorporates alternating window-shaped doping, a graphene grating layer, and strategically positioned gold nanoparticles. This design is evaluated against various configurations, including cells with only window doping, grating, or nanoparticles, and a composite cell integrating all three enhancements. Our analysis reveals that the composite structure significantly increases the electric field strength within the active region, leading to substantial performance improvements.

We employed COMSOL Multiphysics for simulation, focusing on the effects of nanoparticle material, size, and distribution on solar cell performance. Initial simulations with gold nanoparticles were expanded to consider alternative materials like silver, aiming to optimize light absorption and scattering properties. Our results indicate a

pronounced improvement in efficiency and current density with the proposed design, underscoring the impact of integrated plasmonic nanoparticles and graphene grating on solar cell performance.

2. The structure of MGIM waveguide

The proposed structure of the solar cell is depicted in Fig. 1. The figure illustrates the composition of the structure, which includes window-shaped doped regions. Additionally, the structure incorporates a sequence of gold nanoparticles positioned beneath the impurity region and between the vacancy region of the doped window. The lower portion of the silicon region is equipped with a graphene grating, facilitating the positioning of nanoparticles between the window-shaped doping and the graphene grating.

Plasmon nanoparticles induce an augmentation in the distribution of near-field surface plasmon polaritons (SPPs) along the interface, extending towards the far field. Nanoparticles have been observed to improve the field strength within the active region, thereby leading to increased photon absorption and improved efficiency and performance of solar cells. Additionally, the presence of window-shaped regions has been found to enhance light absorption, resulting in a greater overall absorption capacity. The utilization of nanoparticles in the window profile enhances the entrapment, adsorption, and overall efficiency of the solar cell. An additional intriguing method for enhancing the efficiency of solar cells involves the implementation of backside gratings [36-42]. These gratings enable the combination of grating resonances with surface plasmon polariton (SPP) wave excitations. The significant enhancement of surface plasmon polariton (SPP) wave excitation can be achieved through the synergistic effect of grating-nanoparticle combination and window shape doping. The study conducted in reference [32] provides a theatrical demonstration of the enhancement of absorbance and efficiency in silicon solar cells through the excitation of surface plasmon polariton (SPP) waves in compound gratings.

This paper introduces a novel approach to enhance the efficiency of solar cells by utilizing two gratings, namely a doping grating on the top and a graphene grating on the bottom, in conjunction with plasmon nanoparticles made of gold. The primary objective of this approach is to amplify the excitation of surface optical oscillations (SOO) waves, which has not been previously explored in the literature.

To further refine the efficiency and performance of our novel silicon solar cell design, we propose an in-depth investigation into the impact of varying plasmonic nanoparticle materials. The initial simulations and designs incorporated gold nanoparticles due to their well-documented plasmonic properties and compatibility with photovoltaic applications. However, alternative materials such as silver present a compelling avenue for exploration due to their distinct optical properties and plasmonic resonance characteristics, which could potentially offer enhanced light absorption and scattering, leading to improved solar cell performance.

For this purpose, we will employ COMSOL Multiphysics 6, a state-of-the-art simulation software, to model and analyze the effects of substituting gold nanoparticles with silver. This advanced tool allows for precise manipulation of material properties and geometrical configurations, enabling a comprehensive comparison of the optical and electrical behaviors inherent to each nanoparticle material. By systematically varying the material of the nanoparticles, we aim to examine the resultant changes in plasmon resonance, light trapping efficiency, and overall solar cell performance metrics such as current density, open-circuit voltage, fill factor, and efficiency.

Our methodology will involve a detailed parameter sweep, encompassing not only the material of the nanoparticles but also their size, shape, and distribution within the solar cell structure. This rigorous approach ensures that the observed enhancements or detriments in solar cell performance can be directly attributed to the material properties of the nanoparticles, thereby providing a clear basis for selecting the optimal nanoparticle material for our proposed solar cell design.

The expected outcome of this investigation is to identify a nanoparticle material that surpasses the performance of gold nanoparticles in our specific solar cell configuration. Should silver nanoparticles demonstrate superior plasmonic effects and light trapping capabilities, they will be considered for integration into the final solar cell design. This exploration is pivotal for pushing the boundaries of plasmonic solar cell efficiency and represents a crucial step towards realizing high-performance, cost-effective photovoltaic devices.

For simulation of proposed structure, the finite-difference time-domain (FDTD) method is used by solving Maxwell's equation. The perfectly match layer (PML) boundary conditions is also used for bottom and upper side and for side boundaries, periodic boundary conditions are used.

As depicted in Fig. 1, nano-particles added at the middle of the proposed structure between the window shaped regions and graphene grating layer to improve the adsorption rate.

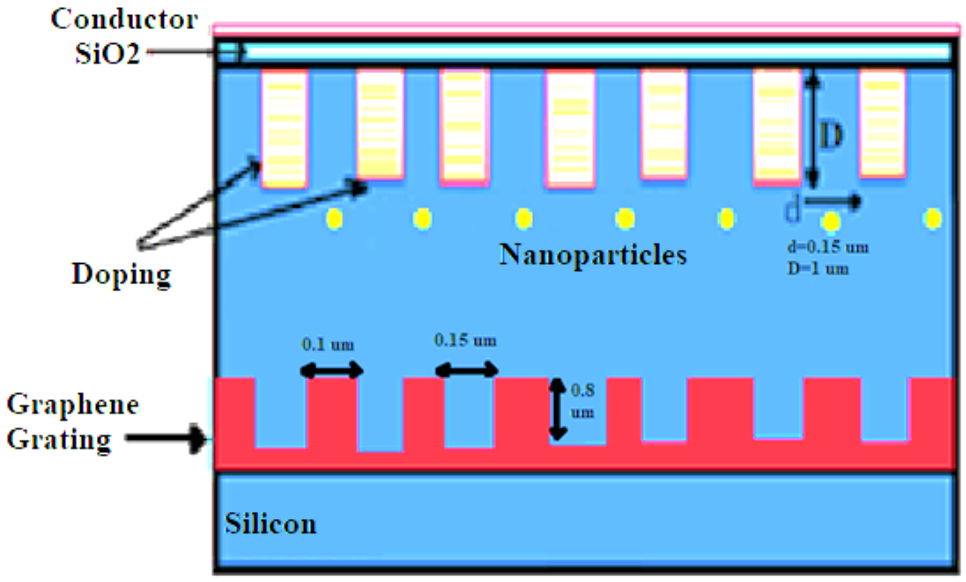

Fig. 1. Structure of the proposed solar cell under consideration (color online)

We assume that a plane field is entered on the desired plane as:

$$\mathbf{E}_{inc}(\mathbf{r},t) = \mathbf{E}_0 e^{j(\mathbf{k}\mathbf{r}_s - \omega t)} \tag{1}$$

If the incoming light is entered at an angle of θ,φ the field in each nanoparticle can be considered as follows:

$$\mathbf{E}_{inc}(\mathbf{r}_s) = \mathbf{E}_0 e^{j\,\mathbf{k}.\mathbf{r}_s} \tag{2}$$

In these relations, the parameters λ r, t, ω, k = ω / c = 2π / λ, c, respectively, are the wavelength of the incoming light, the speed of light, the wave vector, the angular frequency, the time and the position vector. In this regard, the parameter k is also calculated from the following equation:

$$\mathbf{k} = \frac{2\pi}{\lambda}\hat{k} = \frac{2\pi}{\lambda}[\sin(\theta)\cos(\varphi), \sin(\theta)\sin(\varphi), \cos(\theta)] \tag{3}$$

For the input field with polarization P, the intensity of E0 field is equal to:

$$\mathbf{E}_0 = [\sin(\theta - \frac{\pi}{2}).\cos(\varphi), \sin(\theta - \frac{\pi}{2}).\sin(\varphi), \cos(\theta - \frac{\pi}{2})] \tag{4}$$

We also have S for polarization field:

$$\mathbf{E}_0 = [\cos(\phi + \frac{\pi}{2}), \sin(\phi + \frac{\pi}{2}), 0] \tag{5}$$

When a field is applied to a particle, the polarization coefficient α is equal to:

$$\alpha_s = V\varepsilon_0 \frac{\varepsilon_r - 1}{1 + L_1(\varepsilon_r - 1)} \tag{6}$$

In this regard, $\varepsilon_r = \varepsilon_{particle} / \varepsilon_{medium}$, ε0 is the coefficient of passage of free space. Also, V is the nanoparticle volume and L1 is the shape factor. For spherical nanoparticles, the shape coefficient is calculated as follows according to the values of a, b, c:

$$e^2 = 1 - \frac{b^2}{a^2} \quad , \quad f^2 = \frac{b^2}{a^2} - 1$$

$$L_1 = \frac{1+f^2}{f^2}[1 - \frac{1}{f}\tan^{-1}(f)] \qquad oblate\ (a < b)$$

$$L_1 = \frac{1-e^2}{e^2}(-1 + \frac{1}{2e}\ln\frac{1+e}{1-e}) \qquad prolate\ (a > b) \tag{7}$$

Now we can define the electric bipolar vector for each nanoparticle as follows:

$$\mathbf{P}_s = \varepsilon_0 \alpha_s \mathbf{E}_{Loc}(\mathbf{r}_s) \tag{8}$$

In this connection, P_s is the induced dipole moment and E is the electric field of each nanoparticle. Therefore, the field within each nanoparticle depends on two factors. An input field and the second field that is caused by the radiation of other nanoparticles.

The sum of these two field fields makes up each nanoparticle, which is calculated from the following equation [9]:

$$\mathbf{E}_{loc,s} = \mathbf{E}_{inc,s} + \mathbf{E}_{dip,s} = \mathbf{E}_0 e^{j\mathbf{k}\mathbf{r}_s} - \sum_{s \neq h} \mathbf{A}_{s,h}\mathbf{P}_s \tag{9}$$

In this respect, P_s is the same as the dipole moment induced in s. Also, As, h is a 3 × 3 matrix that is calculated as follows.

$$\begin{cases} \mathbf{A}_{s,h}=\dfrac{\exp(j\mathbf{k}\mathbf{r}_{s,h})}{\mathbf{r}_{s,h}}[k^2(r_{sh}r_{sh}\text{-}\mathbf{I}_{3\times3})+\dfrac{jk\mathbf{r}_{sh}-1}{\mathbf{r}_{sh}^2}(3r_{sh}r_{sh}\text{-}\mathbf{I}_{3\times3})] & s\neq h \\ \mathbf{A}_{s,s}=\dfrac{1}{\alpha_s\varepsilon_0\mathbf{I}_{3\times3}} \end{cases} \quad (10)$$

In the third step, the equation must be solved and the vector P calculated from it. In this case, A is a 3N × 3N tensor. The schematic of matrix A is shown in Fig. 2.

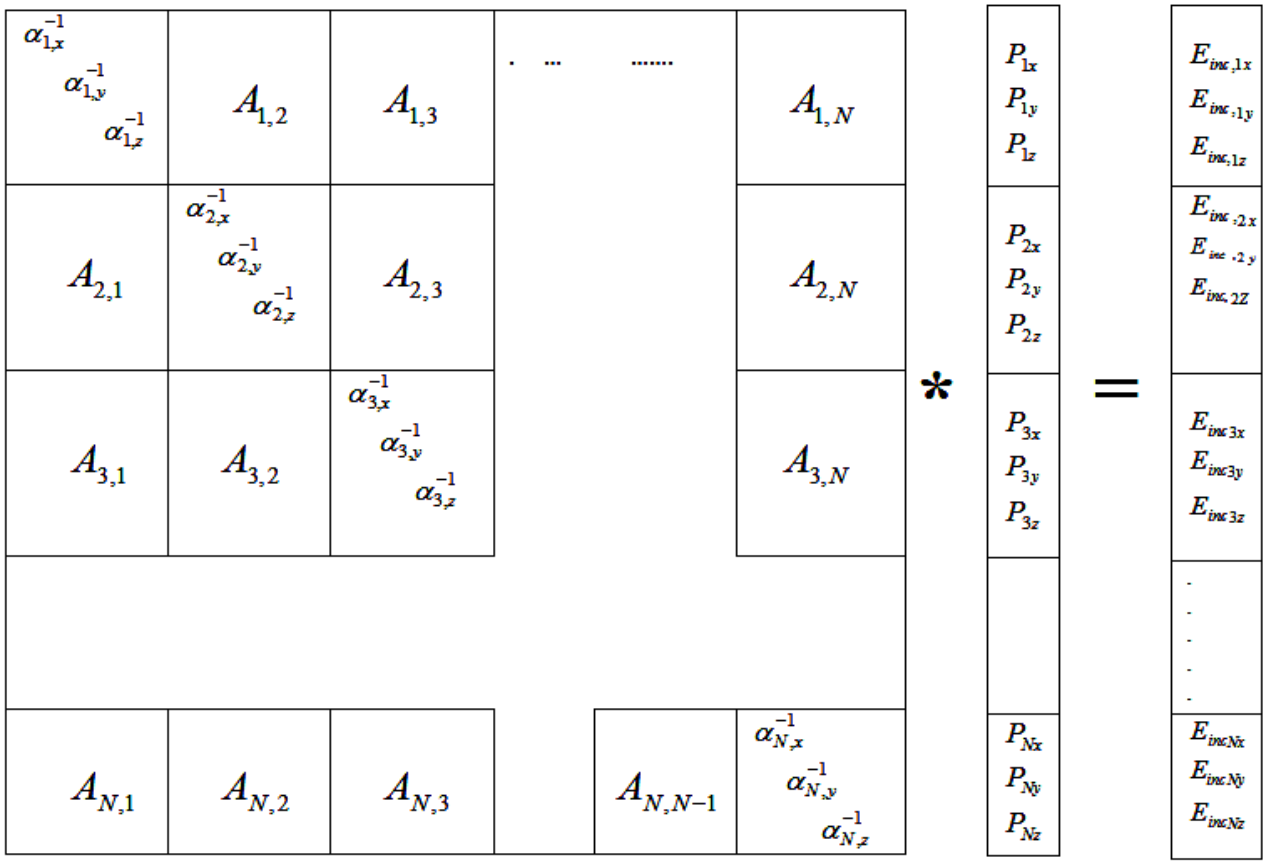

Fig. 2. Schematic of matrix A

In the third step, the equation must be solved and the vector P must be calculated from it. In this relation A is a tensor of order 3N × 3N.

In the fourth step, the absorption (scattering) and scattering (extinction) characteristics should be calculated as follows.

$$Q_{ext}=\frac{k}{\pi a^2\varepsilon_0\left|\overline{E_{inc}}\right|^2}\sum_{i=1}^{N}\mathrm{Im}(\overline{E}_{inc,i}^{*}.\overline{P}_i) \quad (11)$$

$$Q_{sca}=\frac{k^4}{6\pi^2a^2\varepsilon_0^2\left|\overline{E_{inc}}\right|^2}\sum_{i=1}^{N}\left|\overline{E}_{inc,i}^{*}.\overline{P}_i\right|^2 \quad (12)$$

$$\mathrm{Qabs} = \mathrm{Qext} - \mathrm{Qsca} \quad (13)$$

Now that the field distribution and electric bipolar vector is available, the absorption spectra can be calculated as follows.

$$A(\lambda)=\int\frac{1}{2}\frac{real(\vec{\nabla}.P)}{P_{in}}\mathrm{dV} = \int\frac{1}{2}\frac{\omega Im(\varepsilon(r,\omega))|E(r,\omega)|^2}{P_{in}}dV \quad (14)$$

where Pin is the power of incident light, ε is the dielectric constant and ω is the angular frequency. The photocurrent then is obtained from:

$$J_{SC}=q\int\frac{I(\lambda)}{\lambda}A(\lambda)d\lambda \quad (15)$$

where I(λ) is intensity of the incident light.

3. Results and discussion

The optical properties of nanoparticles are highly sensitive to their radius. So, plasmon coupling can be tuned by changing the radius of nanoparticles. In this paper, coupled nanoparticles in different radius are applied

to optimize photocurrent and efficiency. The radius of nanoparticles is selected as 20 nm at first and then they will be optimized to reach the best performance.

Fig. 3 shows the electric field profile of solar cell for different structures. One can see that by adding the window shape doping or nanoparticle, the electric field intensity is increased and the number and peak of its ups and downs is increased. The proposed structure with combination of graphene grating, gold nanoparticles and window shape doping has the highest pick of electric field.

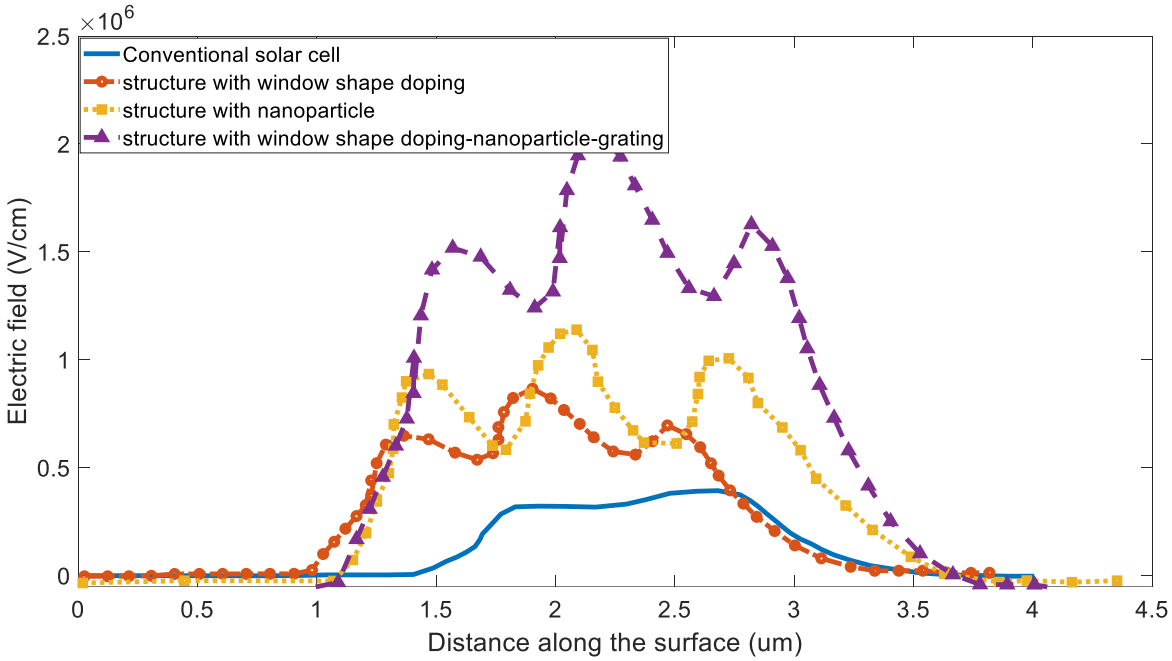

Fig. 3. The electric field profile of solar cell without and with window shape doping (color online)

Field profile modification increases the photon entrapment in the center of the active region. The interaction of these photons with nanoparticles and graphene grating in this region leads to a further increase in field strength and consequently to the performance of the solar cell. External quantum efficiency, current-voltage characteristics of solar cell with different structures are shown in Fig. 4 and Fig. 5, respectively. Performance parameters of electrical simulation including short circuit current, open circuit voltage, fill factor, and efficiency of different structures are summarized in Table 1.

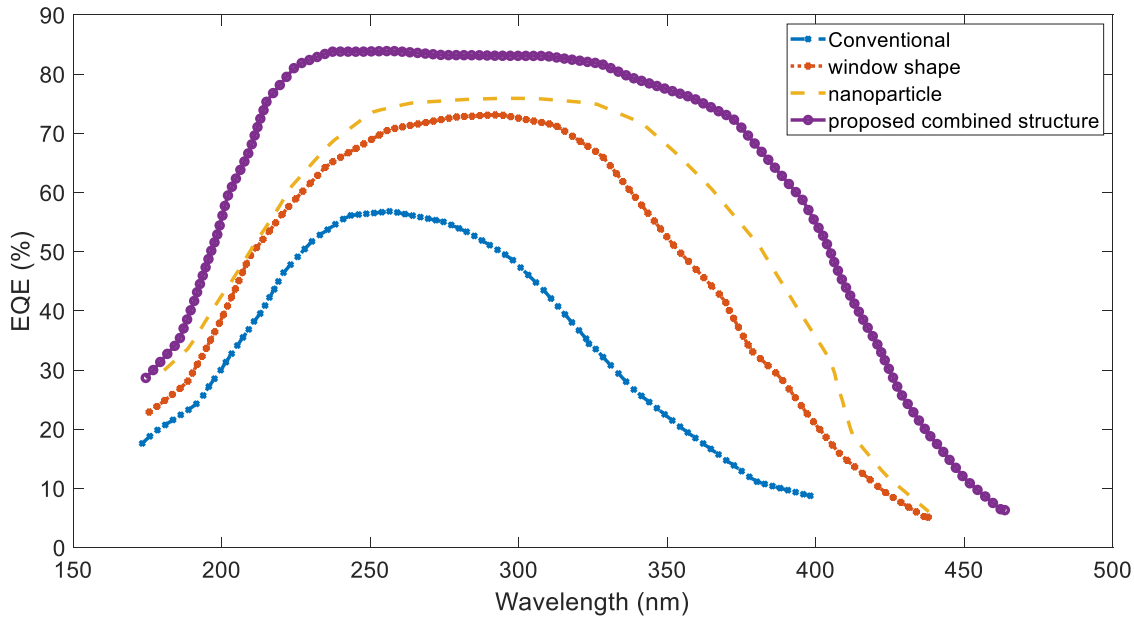

Fig. 4. Comparison of EQE for different structures of solar cells (color online)

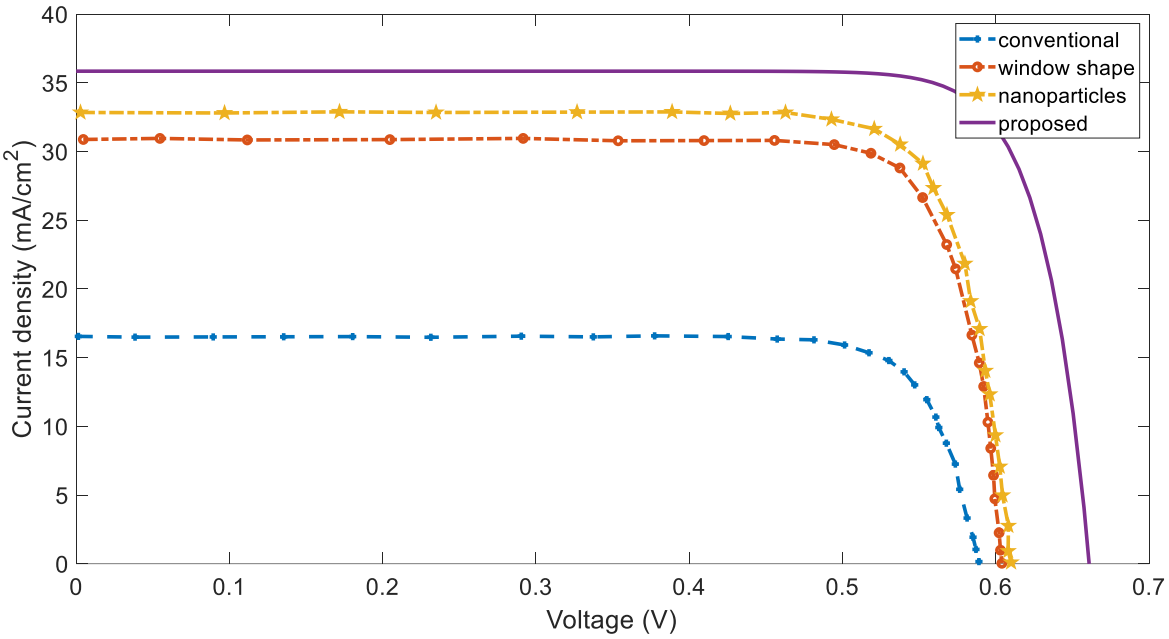

Fig. 5. Comparison of current voltage characteristics for different structures of solar cells (color online)

Table 1. Performance parameters solar cell with different structure

structure	J_{SC}(mA/cm^2)	V_{OC} (v)	FF (%)	Efficiency (%)	EQE (%)
Conventional	16	0.53	0.78	7.4	50
Window shape	30	0.6	0.83	13	69
Nanoparticle	33	0.61	0.82	14	72
Proposed structure	35	0.66	0.83	17	81

As clear from the Figs. 3 and 4 and from Table 1, the addition of window-shaped impurities or gold nanoparticles increases the external quantum efficiency as well as the short-circuit current, the open circuit voltage, and the efficiency. It can also be seen that by combining the window shape doping, grating and nanoparticles leads to a significant increase in these characteristics.

4. Conclusions

This research introduces a novel and optimized structure for plasmonic-based silicon solar cells, designed to significantly enhance external quantum efficiency (EQE), current density, and overall efficiency. The proposed architecture integrates window-shaped doping, an array of plasmonic nanoparticles, and a graphene grating layer, establishing a multifaceted approach to improve solar cell performance. Our findings demonstrate that incorporating nanoparticles or window-shaped doping substantially increases the electric field strength within the active region, thereby leading to notable enhancements in solar cell functionality. Furthermore, the synergistic combination of window-shaped doping, graphene grating, and plasmonic nanoparticles results in a remarkable improvement in solar cell characteristics.

The implementation of this optimized structure has led to an increase in solar cell efficiency up to 17%, marking a significant advancement over previously reported designs. Notably, the proposed structure has achieved more than a 2.5-fold improvement in efficiency. These enhancements are not limited to efficiency alone; substantial gains in fill factor (FF) and EQE were also observed, underscoring the comprehensive impact of the optimized design on solar cell performance. The results of this study clearly indicate that the proposed structure offers a potent solution for achieving high-efficiency plasmonic-based silicon solar cells, paving the way for future advancements in solar energy technology.

References

[1] S. S. Bagade, S. Patel, M. M. Malik, P. K. Patel, C Journal of Carbon Research **9**, 70 (2023).
[2] D. Adabi, M. R. Moslemi, M. R. Shayesteh, S. Hashemian, Optoelectron. Adv. Mat. **16**(3-4), 142 (2022).

[3] S. R. Mirnaziry, M. A. Shameli, L. Yousefi, Sci. Rep. **12**, 13259 (2022).
[4] A. S. M. Mohsin, S. Mondal, M. Mobashera, A. Malik, M. Islam, M. Rubaiat, Heliyon **9**(6), e16749 (2023).
[5] H. Soonmin, Hardani, P. Nandi, B. S. Mwankemwa, T. D. Malevu, M. I. Malik, Appl. Sci. **13**, 2051 (2023).
[6] C. F. Bohren, D. R. Huffman, Absorption and Scattering of Light by Small Particles Wiley, New York, 1983.
[7] H. Masuda, M. Satoh, Jpn. J. Appl. Phys., Part 2, **35**, L126 (1996).
[8] M. L. Brongersma, Y. Cui, S. Fan, Nat. Mater. **13**, 451 (2014).
[9] V. E. Ferry, M. A. Verschuuren, H. B. T. Li, R. E. I. Schropp, H. A. Atwater, A. Polman, Appl. Phys. Lett. **95**, 183503 (2009).
[10] F. J. Beck, S. Mokkapati, K. R. Catchpole, Prog. Photovolt. Res. Appl. **18**, 500 (2010).
[11] Z. Ouyang, S. Pillai, F. J. Beck, O. Kunz, S. Varlamov, K. R. Catchpole, P. Campbell, M. A. Green, Appl. Phys. Lett. **96**, 261109.1 (2010).
[12] X. Chen, B. H. Jia, J. K. Saha, B. Y. Cai, N. Stokes, Q. Qiao, Y. Q. Wang, Z. R. Shi, M. Gu, Nano Lett. **12**, 2187 (2012).
[13] N. Fahim, Z. Ouyang, Y. N. Zhang, B. Jia, Z. R. Shi, M. Gu, Opt. Mater. Express **2**, 190 (2012).
[14] Y. N. Zhang, Z. Ouyang, N. Stokes, B. H. Jia, Z. R. Shi, M. Gu, Appl. Phys. Lett. **100**, 151101.1 (2012).
[15] D. M. Schaadt, B. Feng, E. T. Yu, Appl. Phys. Lett. **86**, 063106.1 (2005).
[16] D. Derkacs, S. H. Lim, P. Matheu, W. Mar, E. T. Yu, Appl. Phys. Lett. **89**, 093103.1 (2006).
[17] J. L. Wu, F. C. Chen, Y. S. Hsiao, F. C. Chien, P. L. Chen, C. H. Kuo, M. H. Huang, C. S. Hsu, ACS Nano **5**, 959 (2011).
[18] N. F. Fahim, B. H. Jia, Z. R. Shi, M. Gu, Opt. Express **20**, A694 (2012).
[19] V. E. Ferry, M. A. Verschuuren, M. C. Van Lare, R. E. I. Schropp, H. A. Atwater, A. Polman, Nano Lett. **11**, 4239 (2011).
[20] T. L. Temple, G. D. K. Mahanama, H. S. Reehal, D. M. Bagnall, Sol. Energy Mater. Sol. Cells **93**, 1978 (2009).
[21] N. Fahim, Z. Ouyang, B. Jia, Y. Zhang, Z. Shi, M. Gu, Appl. Phys. Lett. **101**, 261102 (2012).
[22] B. Cai, N. Stokes, B. Jia, M. Gu, Appl. Phys. Lett. **102**, 093107 (2013).
[23] W. Yan, N. Stokes, B. Jia, M. Gu, Opt. Lett. **15**, 395 (2013).
[24] X. Chen, B. H. Jia, J. K. Saha, N. Stokes, Q. Qiao, Y. Q. Wang, Z. R. Shi, M. Gu, Opt. Mater. Express **3**, 27 (2013).
[25] N. Stokes, B. H. Jia, M. Gu, Appl. Phys. Lett. **101**, 141112.1 (2012).
[26] K. Nakayama, K. Tanabe, H. A. Atwater, Appl. Phys. Lett. **93**, 121904 (2008).
[27] S. Pillai, K. R. Catchpole, T. Trupke, M. A. Green, J. Appl. Phys. **101**, 093105 (2007).
[28] F. J. Beck, A. Polman, K. R. Catchpole, J. Appl. Phys. **105**, 114310 (2009).
[29] S. S. Kim, S. I. Na, J. Jo, D. Y. Kim, Y. C. Nah, Appl. Phys. Lett. **93**, 073307 (2008).
[30] Y. A. Akimov, W. S. Koh, Nanotechnology **21**, 235201 (2010).
[31] Z. Sun, X. Zuo, Y. Yang, Opt. Lett. **37**, 641 (2012).
[32] M. R. M. Atalla, J. Opt. Soc. Am. B **31**, 1906 (2014).
[33] P. Prabhathan, V. M. Murukeshan, Plasmonics **11**, 253 (2016).
[34] Vivian E. Ferry, Luke A. Sweatlock, Domenico Pacifici, Harry A. Atwater, Nano Lett. **8**, 4391 (2008).
[35] L. V. Mercaldo, I. Usatii, E. Bobeico, F. Russo, L. Lancellotti, P. Delli Veneri, Energy Procedia **84**, 221 (2015).
[36] J. Chantana, Y. Q. Yang, Y. Sobajima, C. Sada, A. Matsuda, H. Okamoto, J. Non-Cryst. Solids **358**, 2319 (2012).
[37] J. Weickert, R. B. Dunbar, H. C. Hesse, W. Wiedemann, L. Schmidt-Mende, Adv. Mater. **23**, 1810 (2011).
[38] L. Lu, Z. Luo, T. Xu, L. Yu, Nano Lett. **13**, 59 (2013).
[39] W. Zhang, M. Saliba, S. D. Stranks, Y. Sun, X. Shi, U. Wiesner, H. J. Snaith, Nano Lett. **13**, 4505 (2013).
[40] D. M. Callahan, J. N. Munday, H. A. Atwater, Nano Lett. **12**, 214 (2011).
[41] J. N. Munday, H. A. Atwater, Nano Lett. **11**, 2195 (2011).
[42] M. G. Deceglie, V. E. Ferry, A. P. Alivisatos, H. A. Atwater, Nano Lett. **12**, 2894 (2012).

*Corresponding author: m_shayesteh45@yahoo.com